Supporting Information

Electronic Engineering of Ni_3S_2 via Mo/Cl Co-doping for Upcycling Polyethylene Terephthalate into Formate with Concurrent Hydrogen Evolution

Guoen Zhang,†[a] Chuanshun Feng,†[a] Feng Lin,[a] Huan Ye,[a] Wenqi Wei,[a] Qicheng Zhang,[a] Xiaobin Fan,[ab] Wenchao Peng [ab] and Yang Li *[ab]

[a] School of Chemical Engineering and Technology, State Key Laboratory of Chemical Engineering and Low-Carbon Technology, Collaborative Innovation Center of Chemical Science and Engineering, Tianjin University, Tianjin 300354, China

[b] Zhejiang Institute of Tianjin University, Shaoxing, Zhejiang 312300, China

† These two authors contributed equally to this work

*Corresponding author, E-mail: liyang1895@tju.edu.cn

S1. Techno-economic assessment

The calculation process as follows:

(1) Input chemicals costs:

The costs associated with the required input chemicals are calculated as follows:1 ton PET (390 \$/t)[1], 1.13 tons KOH (1126 \$/t)[2], 10 tons water (0.22 \$/t)[3] and 0.53 tons formic acid (400 \$/t)[4].

Thus, the input chemicals is:

Costs = (1 × 390) + (1.13 × 1126) + (10 × 0.22) + (0.53 × 400) = 1876.6 \$

(2) Electricity costs:

The total charge required for electrochemical PET upgrading per ton is determined by:

$$Q = \frac{N \times F \times n}{FE} = \frac{4770 \times 96485 \times 6}{0.82} = 3.36 \times 109\ \mathrm{C}$$

Where Q is the total charge, N is the moles of EG per ton of PET, F is the Faraday constant (96485 C mol^{-1}), n is the number of electron transfer (6), and FE is the Faradaic efficiency of formate production.

The power consumption is then calculated as:

$$P = \frac{U \times Q}{3600 \times f} = \frac{1.61 \times 3.36 \times 109}{3600 \times 0.8} = 1878.3\ kWh$$

Where U is the cell potential (1.61 V), f is a capacity factor (0.8). Assuming an electricity price of 0.07 \$/kWh, the electricity cost amounts to:

Electricity costs = 1878.3 × 0.07 = 131.4 \$

(3) Separation and purification costs

Separation and purification costs, estimated as 20% of the electricity costs, are given by:

Separation and purification cost = 131.4 × 0.2=26.3 \$

(4) Miscellaneous costs

Miscellaneous costs, covering capital costs, Installation costs, balance of plant, operational costs, and maintenance costs, are estimated at 10% of the total costs

incurred thus far:

Miscellaneous cost = (1876.6 + 131.4 + 26.3) ×0.1 = 203.4 $

(5) Total cost of PET upcycling:

Total cost = 1876.6 + 131.4 + 26.3 + 203.4 = 2237.7 $

(6) After electrolysis, 1 ton of PET feedstock finally yields 1.67 tons of HCOOK (852 $/t)[5], 0.84 tons of TPA (1260 $/t)[6] and 0.037 tons of H_2 (4800 $/t)[5].

The corresponding product value is:

Product value = (1.67 × 852) + (0.84 × 1260) + (0.037 × 4800) = 2658.8 $

The net profit from electrolysis per ton of PET is calculated as:

Total profit = Product value − Total Cost = 2658.8 −2237.7 = 421.1 $

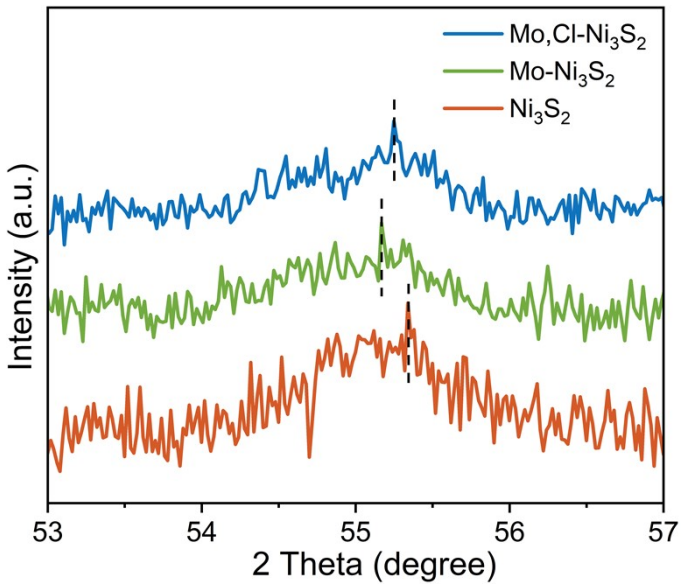

Fig. S1 XRD patterns of Mo,Cl-Ni_3S_2, Mo-Ni_3S_3 and Ni_3S_2.

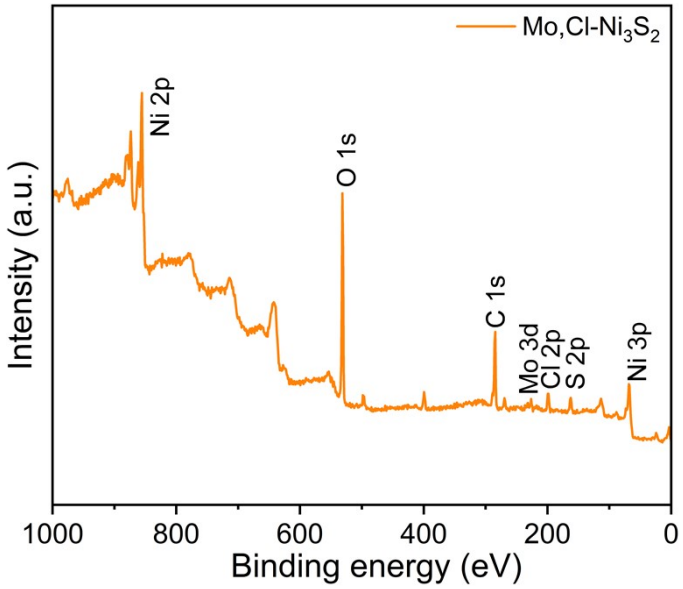

Fig. S2 XPS survey spectrum of Mo,Cl-Ni_3S_2.

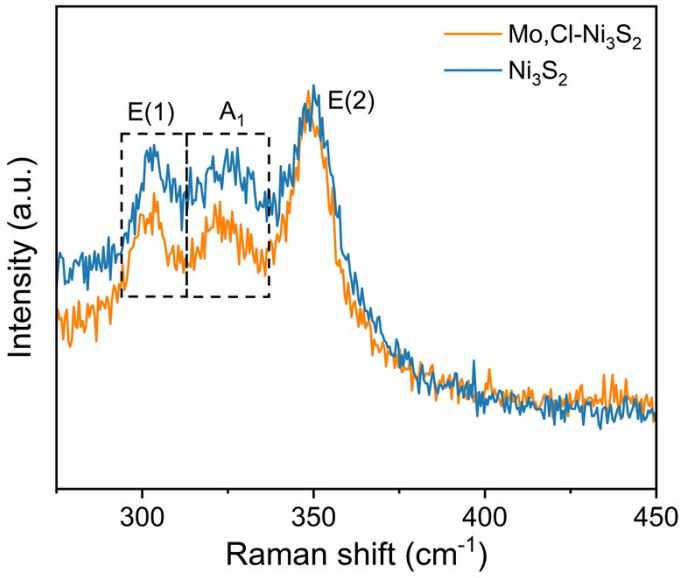

Fig. S3 Raman spectra of Mo,Cl-Ni_3S_2 and Ni_3S_2.

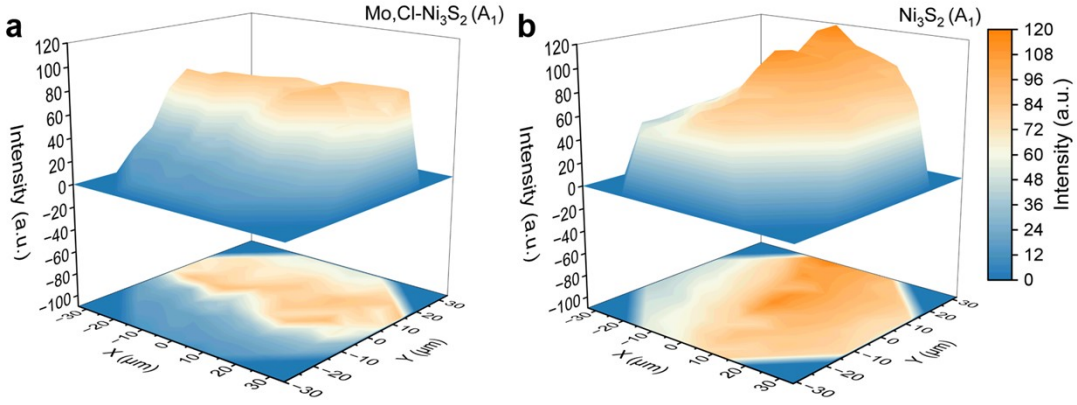

Fig. S4 Raman spectra heatmap of the A_1 vibrational mode of (a) Mo,Cl-Ni_3S_2 and (b) Ni_3S_2.

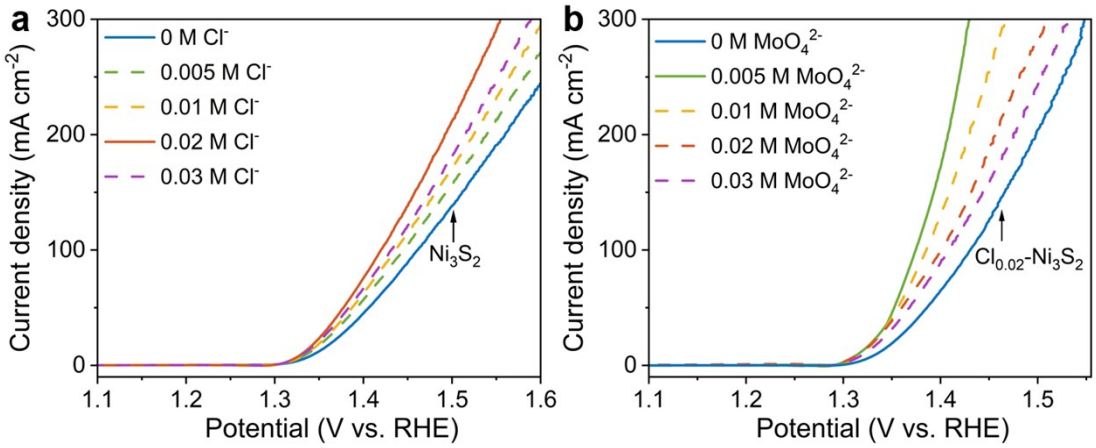

Fig. S5 (a) Effect of Cl^- doping level on the catalytic performance of Ni_3S_2. (b) Effect of MoO_4^{2-} doping level on the catalytic performance of $Cl_{0.01}$-Ni_3S_2 ($Cl_{0.01}$ means the dosage of Cl^- precursor is 0.01 M).

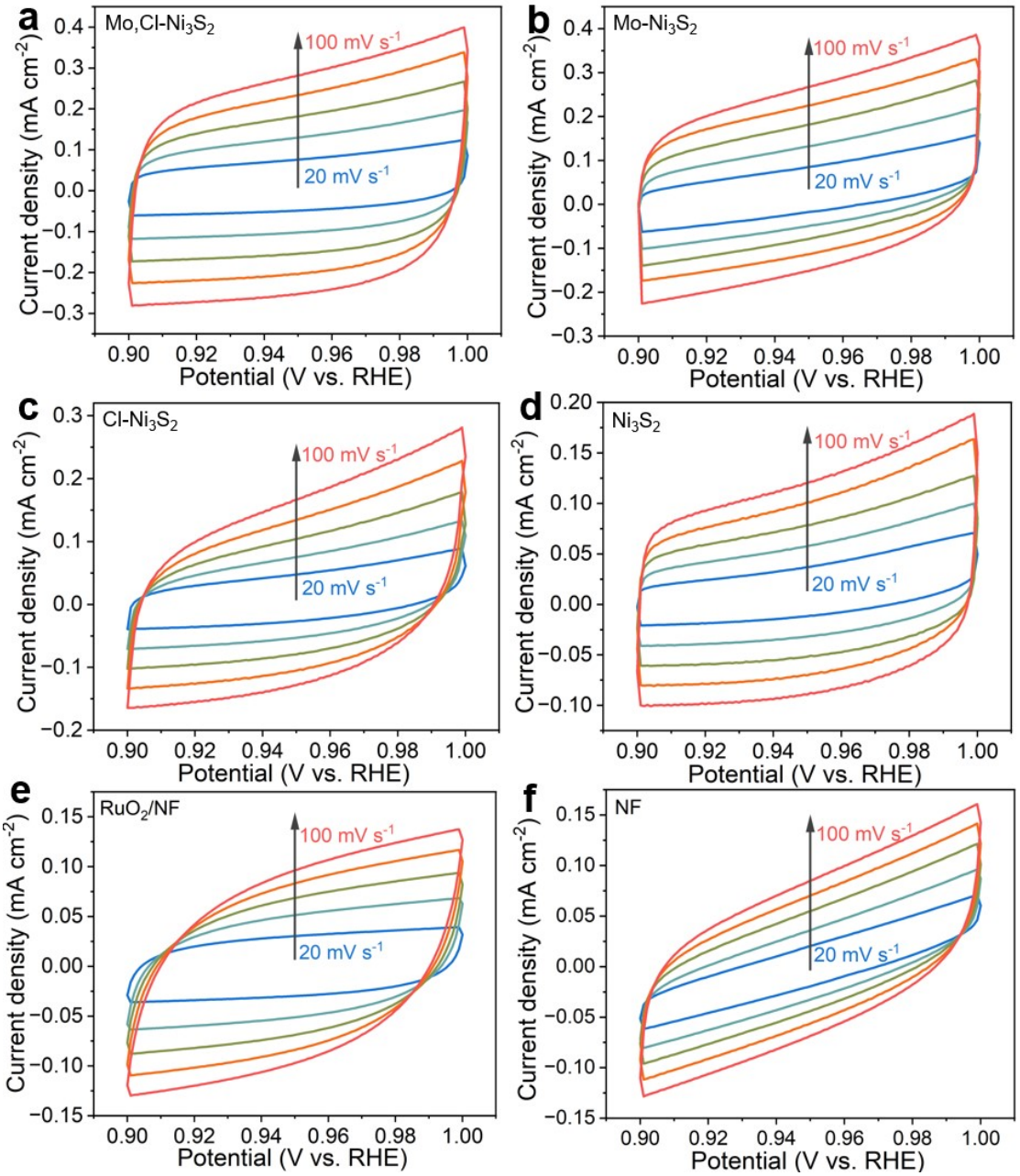

Fig. S6 CV of (a) Mo,Cl-Ni_3S_2, (b) Mo-Ni_3S_2, (c) Cl-Ni_3S_2, (d) Ni_3S_2 (e) RuO_2/NF and (f) NF at different scan rates (from 20 to 100 mV s^{-1} with an increment of 20 mV s^{-1}).

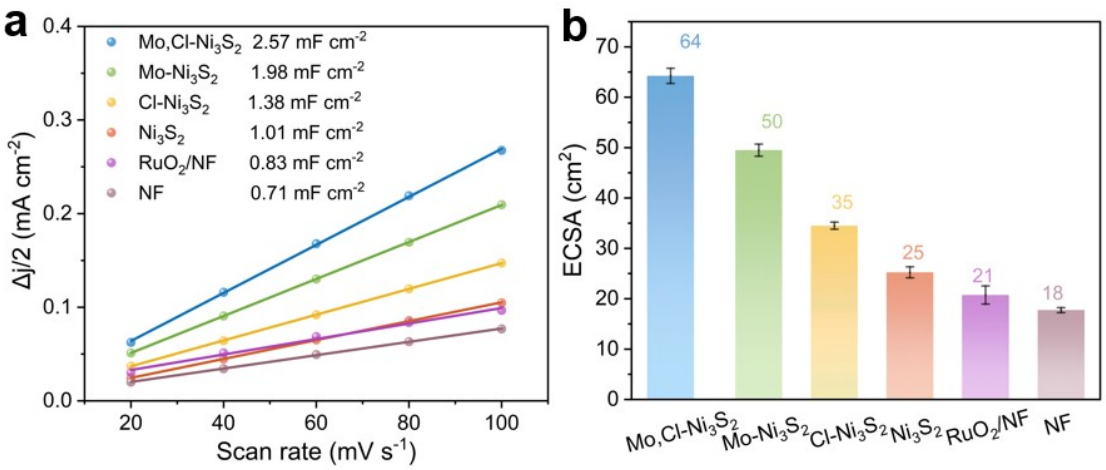

Fig. S7 (a) The difference in current density ($\Delta j = (ja – jc)/2$) plots against the scan rate of Mo,Cl-Ni_3S_2, Mo-Ni_3S_2, Cl-Ni_3S_2, Ni_3S_2, RuO_2/NF and NF. (b) ECSA values of catalysts.

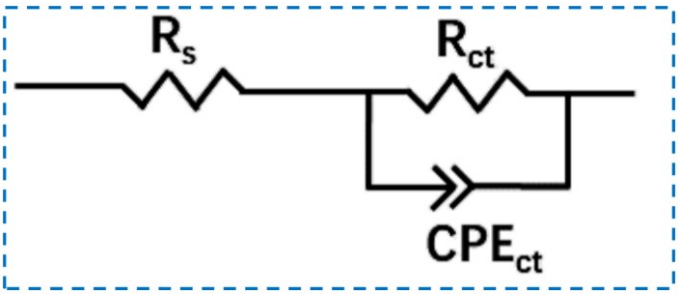

Fig. S8 Equivalent circuit model for EIS data fitting.

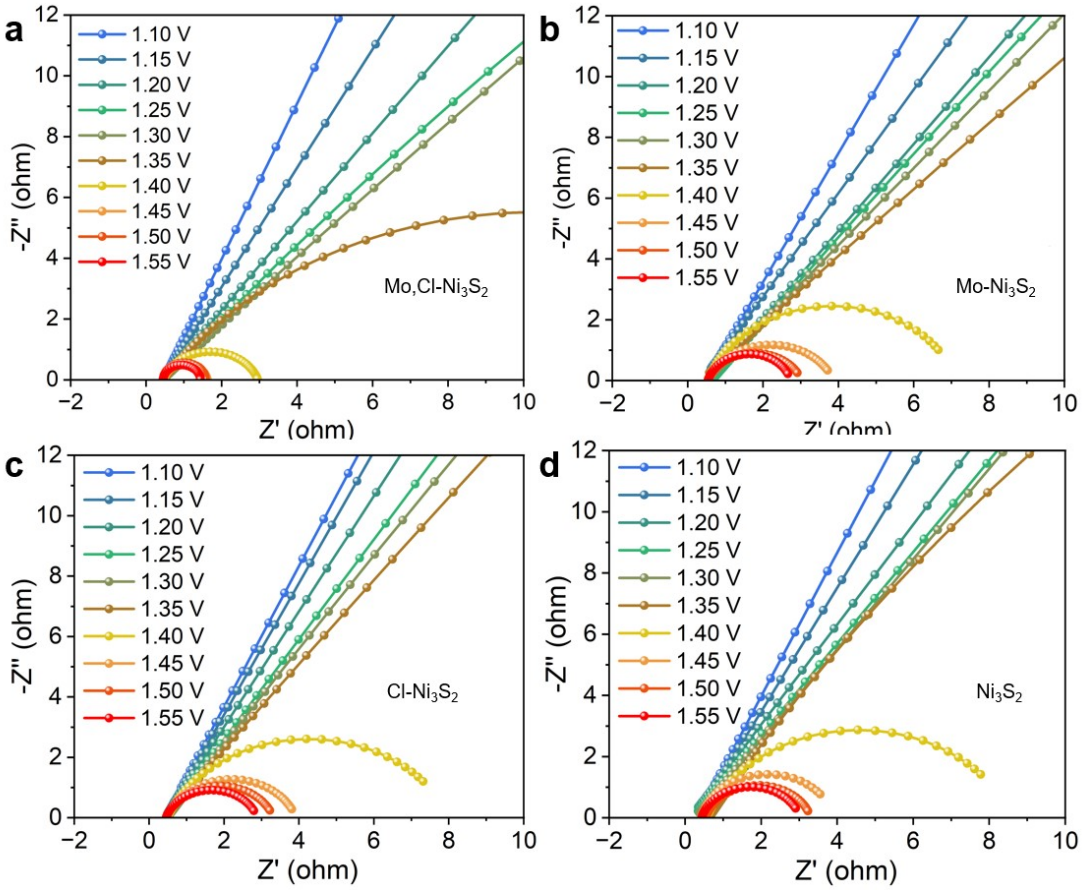

Fig. S9 Nyquist plots of (a) Mo,Cl-Ni_3S_2, (b) Mo-Ni_3S_2, (c) Cl-Ni_3S_2, and (d) Ni_3S_2.

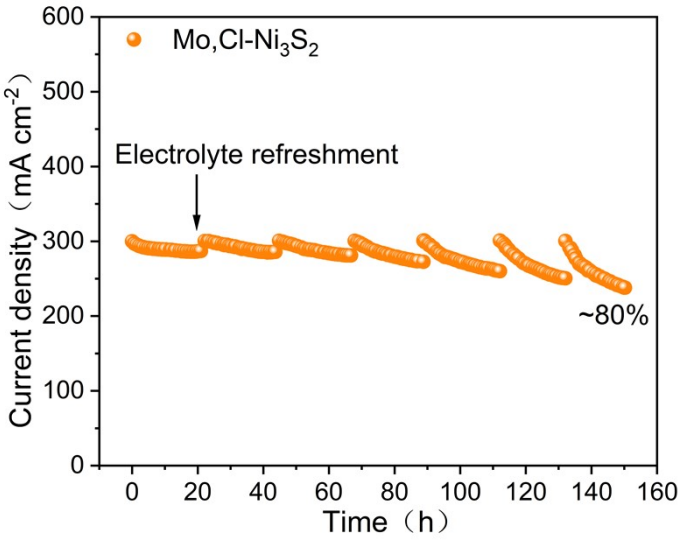

Fig. S10 The chronoamperometric curves of Mo,Cl-Ni_3S_2 for the 150 h EGOR test.

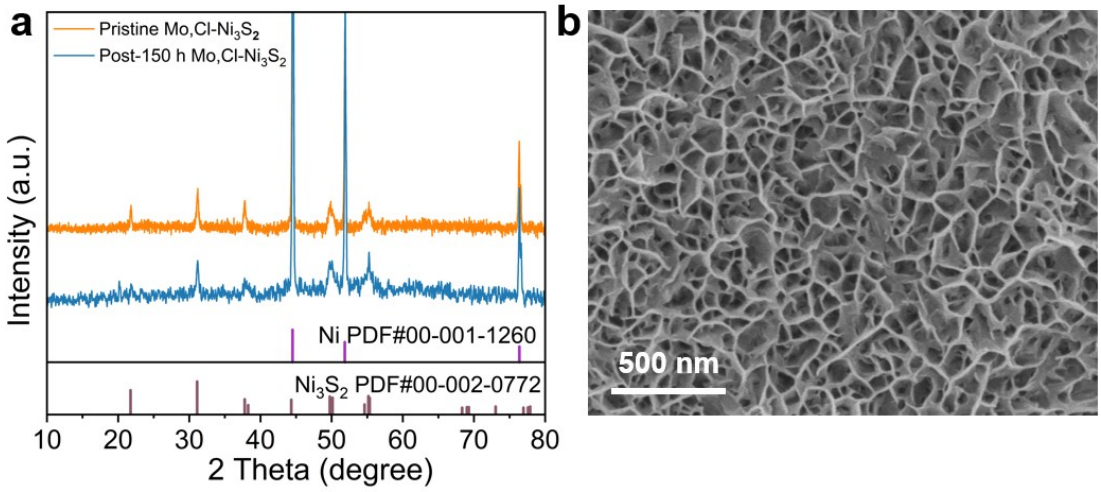

Fig. S11 (a) XRD and (b) SEM images of Mo,Cl-Ni_3S_2 after 150 h stability test.

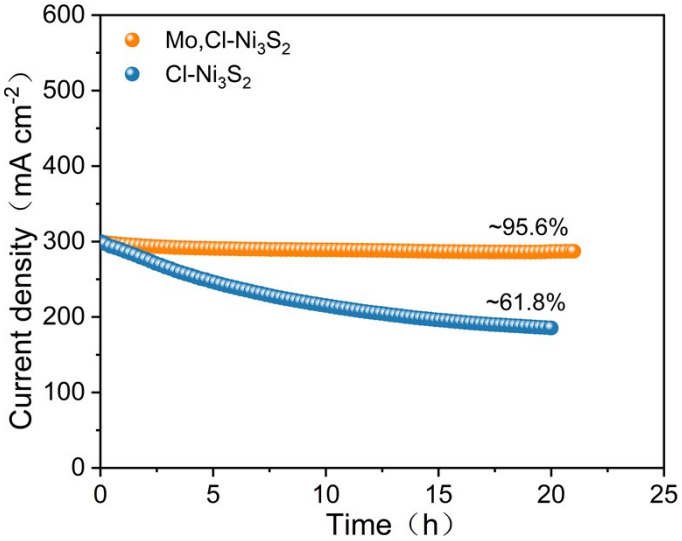

Fig. S12 Comparison of the long-term stability between Mo,Cl-Ni_3S_2 and Cl-Ni_3S_2.

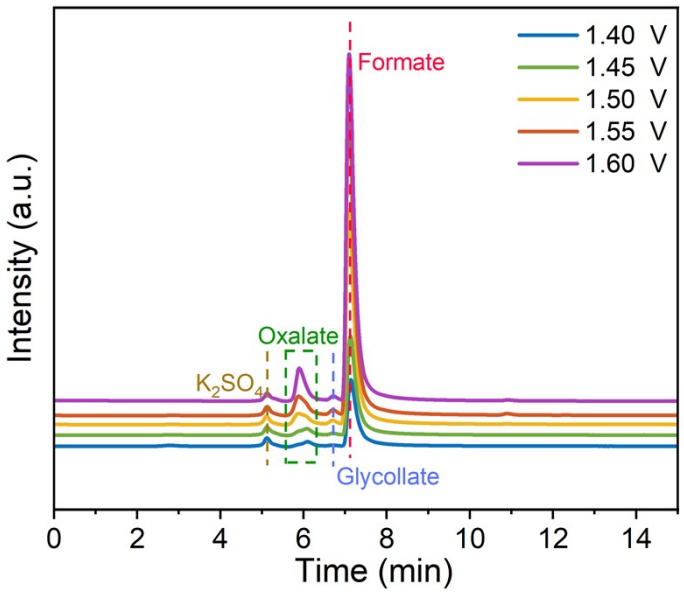

Fig. S13 HPLC products of EGOR at different potentials.

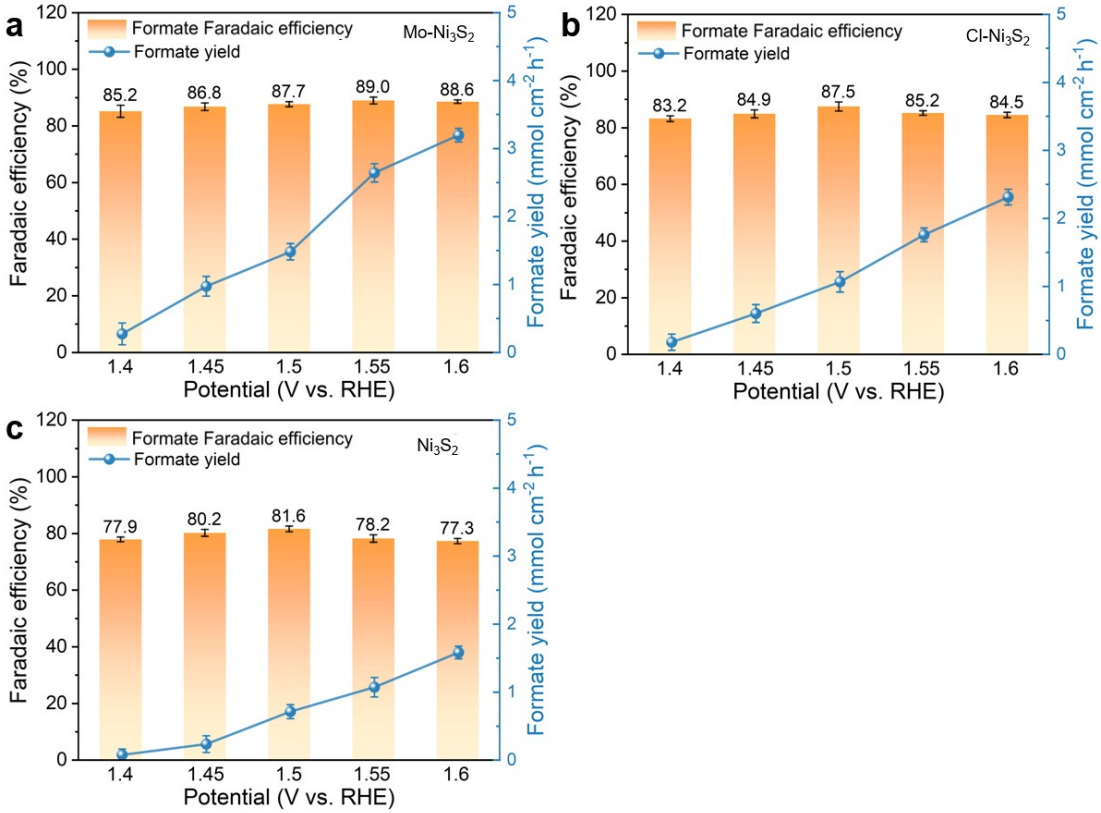

Fig. S14 Faradaic efficiency and yield for formate production of (a) Mo-Ni_3S_2, (b) Cl-Ni_3S_2, and (c) Ni_3S_2 at different potentials.

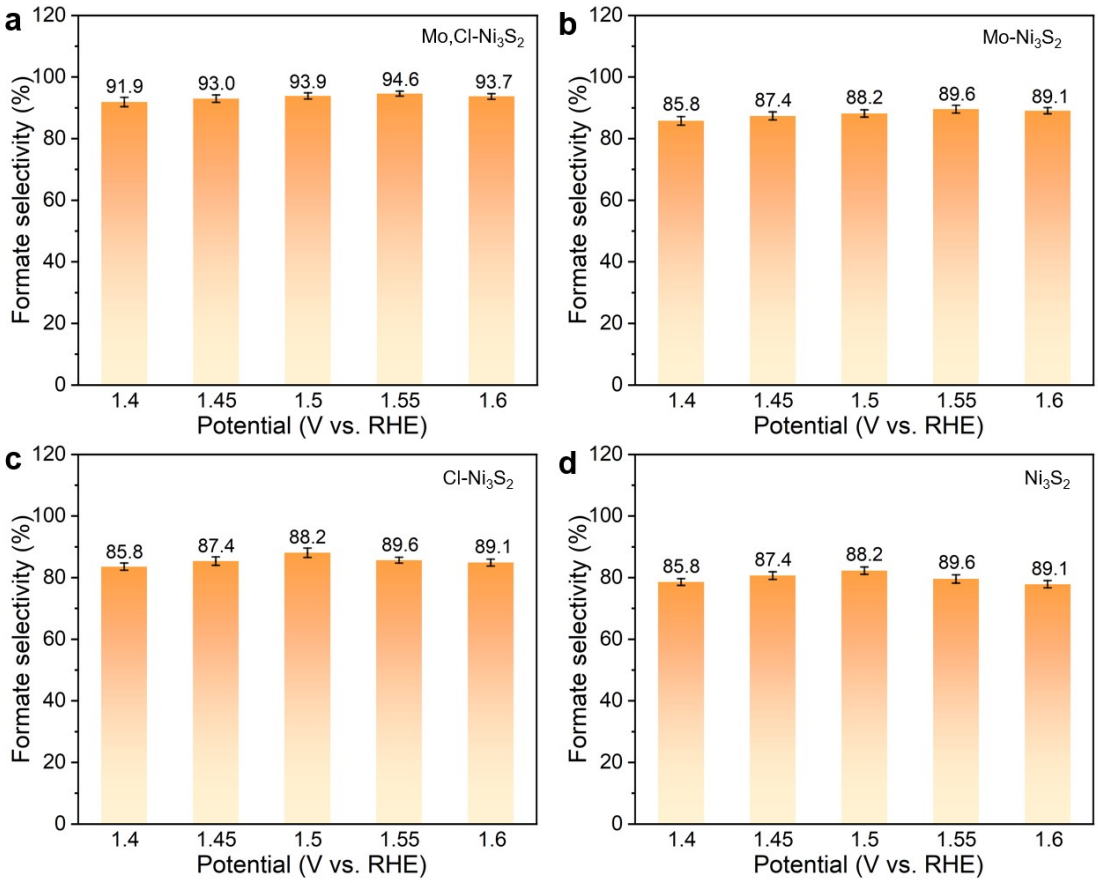

Fig. S15 Formate selectivity of (a) Mo,Cl-Ni_3S_2, (b) Mo-Ni_3S_2, (c) Cl-Ni_3S_2, and (d) Ni_3S_2 at varied applied voltages.

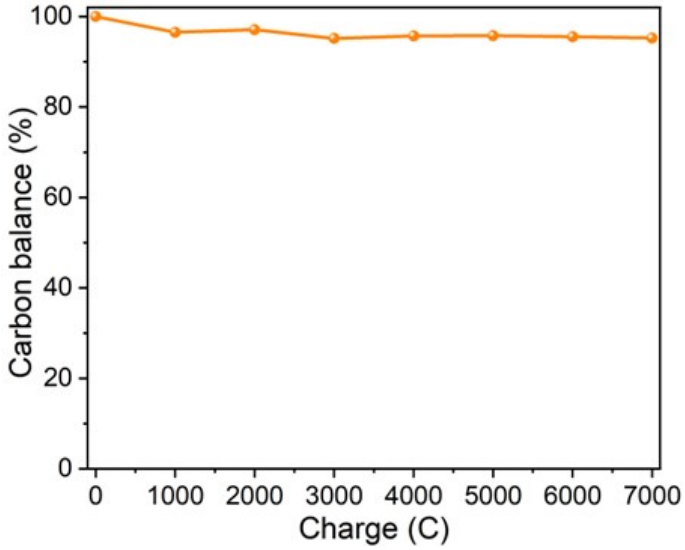

Fig. S16 Carbon balance of EGOR at different input charges.

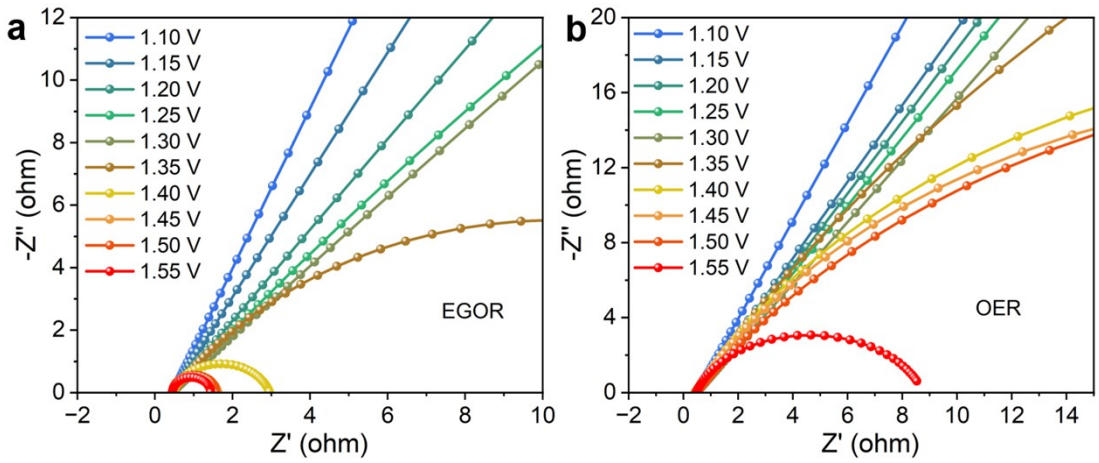

Fig. S17 Nyquist plots of Mo,Cl-Ni_3S_2 for (a) OER and (b) EGOR.

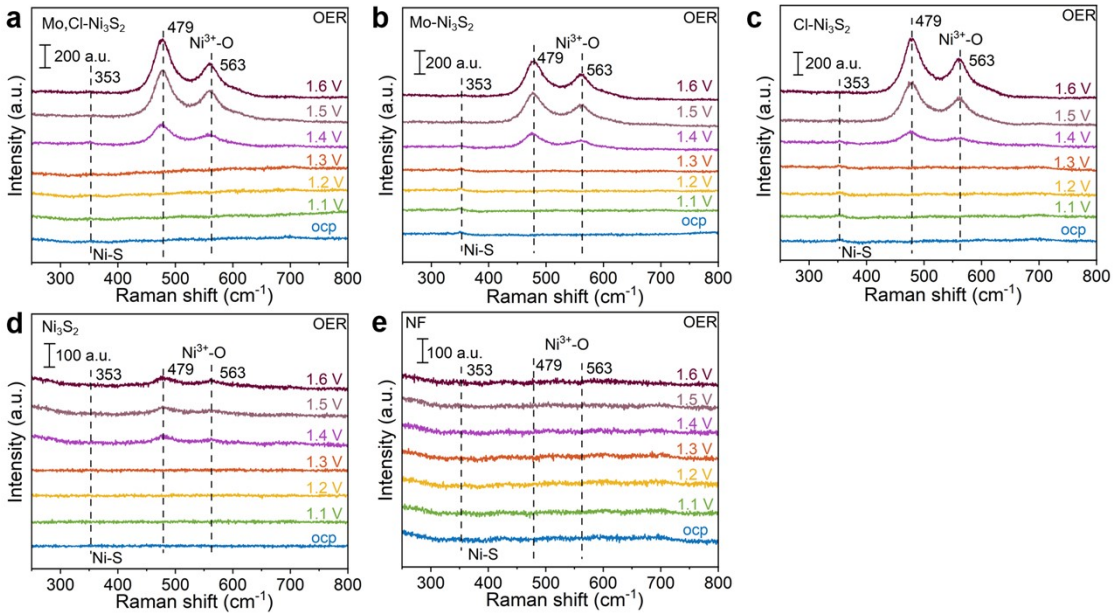

Fig. S18 *In situ* Raman spectra of (a) Mo,Cl-Ni_3S_2, (b) Mo-Ni_3S_2, (c) Cl-Ni_3S_2, (d) Ni_3S_2, and (e) Ni_3S_2.

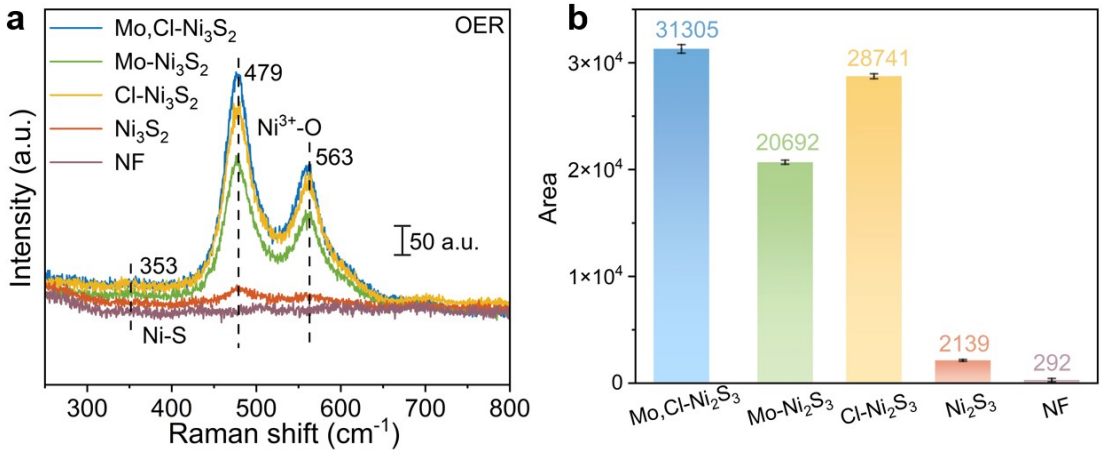

Fig. 19 (a) Comparison of *in situ* Raman peaks at 1.5 V vs. RHE. (b) The corresponding Raman peak area of NiOOH at 1.5 V vs. RHE.

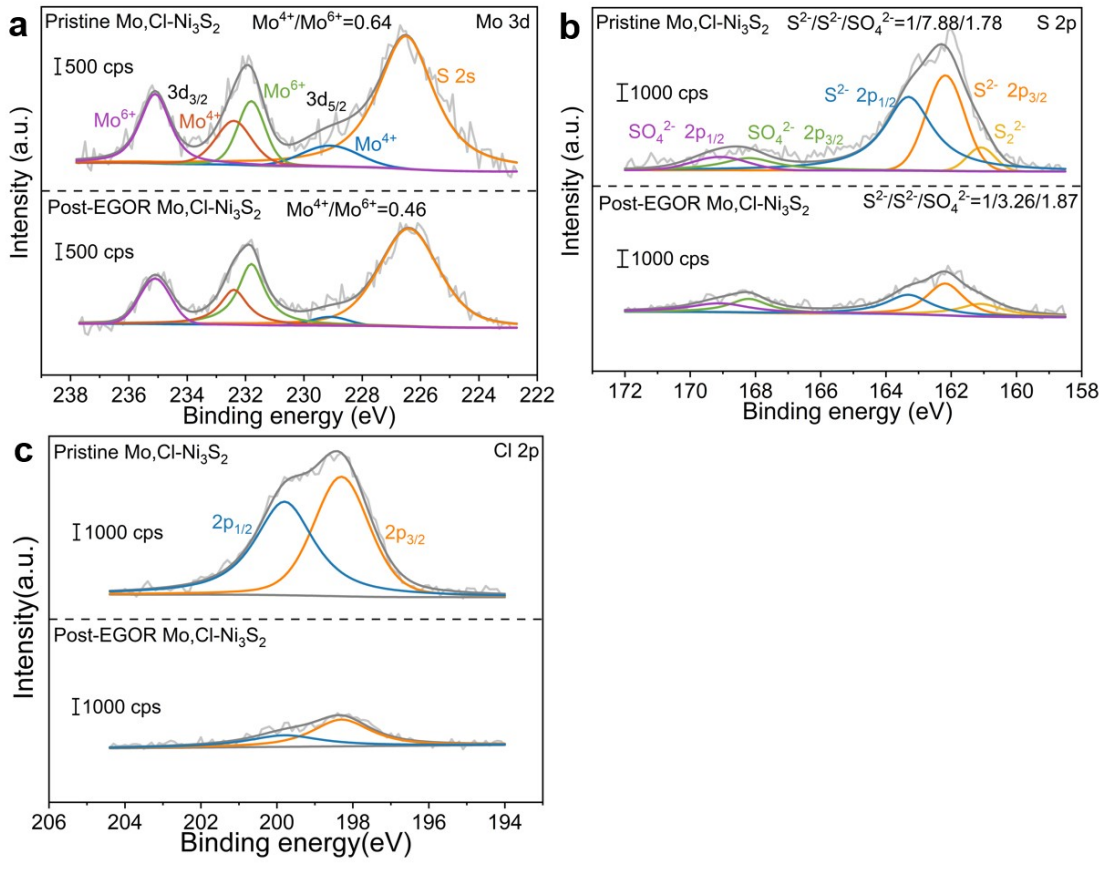

Fig. S20 (a) Mo 3d, (b) S 2p and (c) Cl 2p XPS spectra of Mo,Cl-Ni_3S_2 before and after EGOR process.

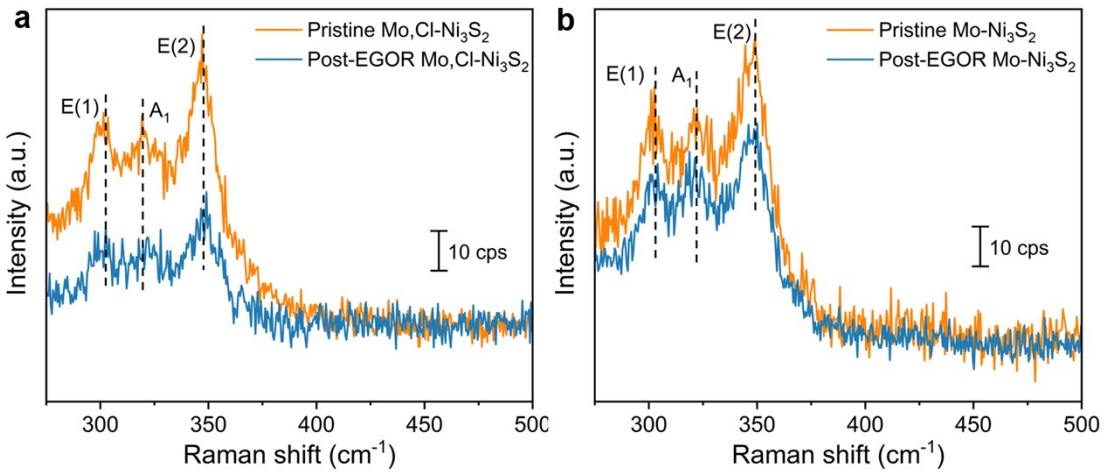

Fig. S21 Raman spectra of (a) Mo,Cl-Ni_3S_2 and (b) Mo-Ni_3S_2 before and after EGOR process.

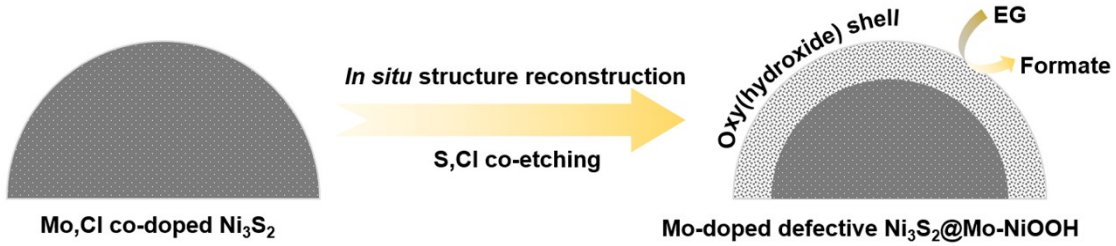

Fig. S22 Illustration of the self-reconstruction process of Mo,Cl-Ni_3S_2.

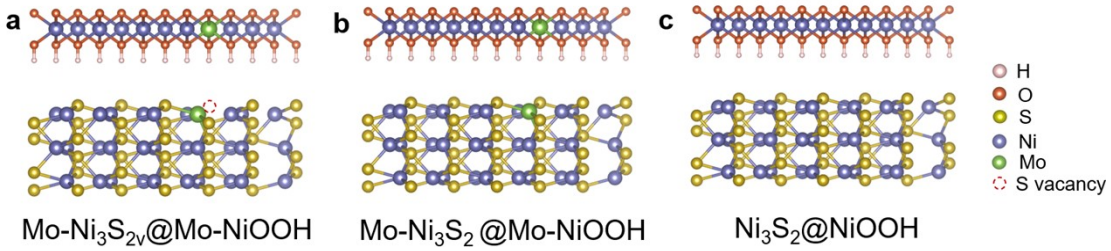

Fig. S23 Constructed (a) Mo-Ni_3S_{2v}@Mo-NiOOH, (b) Mo-Ni_3S_2@Mo-NiOOH, and (c) Ni_3S_2@NiOOH models for DFT calculations. Since Cl is a dopant and replace some S sites in the Ni_3S_2 crystal structure, the electrochemical etching of Cl will thus lead to S vacancy.

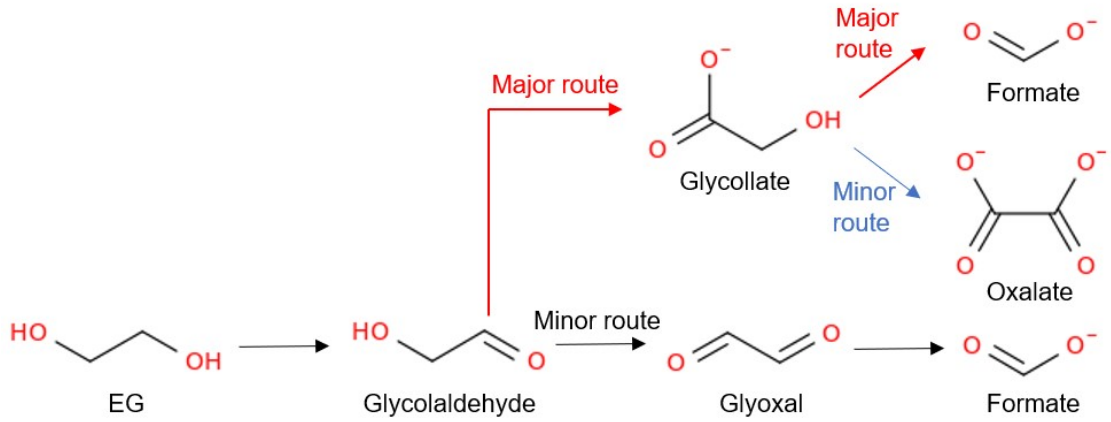

Fig. S24 Proposed reaction pathway for the electrocatalytic glycol conversion.

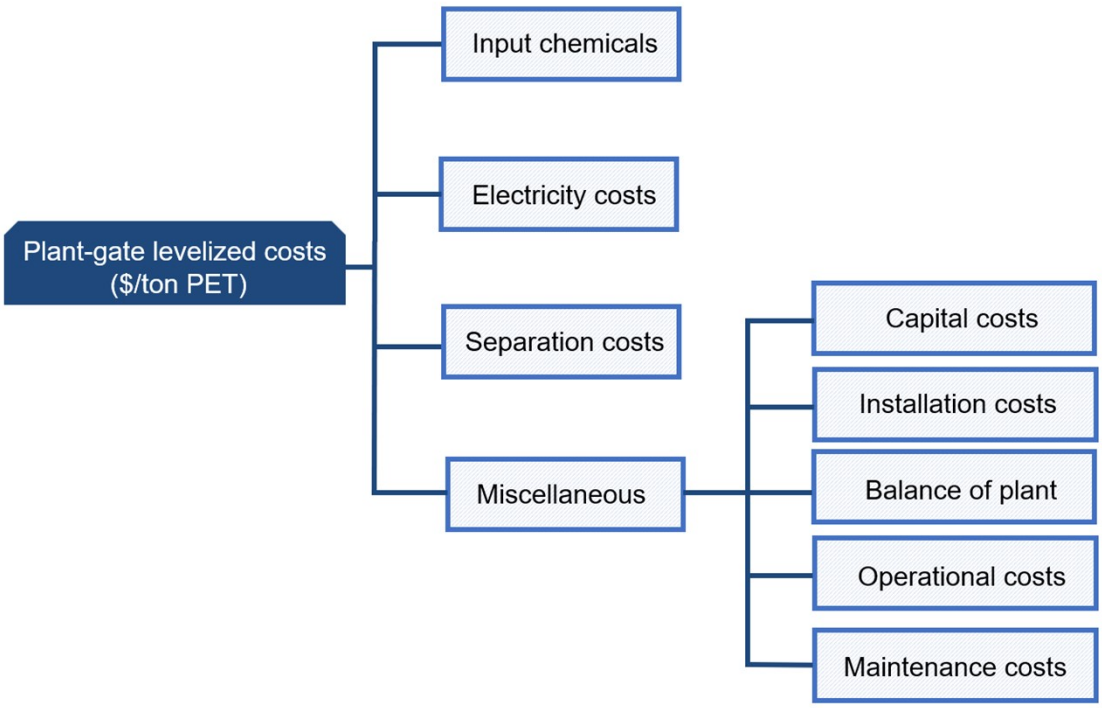

Fig. S25 The costs for calculating techno-economic analysis of electrolytic PET wastes conversion.

Table S1 A summary of OER properties of Mo,Cl-Ni_3S_2 and state-of-the-art TM-based catalysts in 1 M KOH.

Catalyst	η_{10} (mV)	References
CoMnOOH	256	*Angew. Chem. Int. Ed., 2024, 63, e202408005.*
MEC-2	258	*Nat. Commun., 2025, 16:4389.*
FeCoSx-PBA	266	*J. Mater. Chem. A, 2022, 10, 19757-19768.*
CoNiSx/NF	306	*ACS Appl. Nano Mater., 2024, 7, 9062-9067.*
CeO_2 (Co_3O_4/CeO_2)	297	*Dalton Trans., 2024, 53, 5484-5494.*
CoFeBTC-MOF	261	*Colloids Surf., A 2022, 651, 129766.*
$Ni_{2.5}Co_5C_2O_4$	330	*Nanoscale Adv., 2021, 3, 3770-3779.*
$Ni_{0.8}Fe_{0.2}$	264	*Langmuir, 2025, 41, 23621-23631.*
$Co_{0.6}Fe_{0.4}C_2O_4$	292	*ACS Appl. Mater. Interfaces, 2025, 17, 46874-46886.*
RuO_x/γ-MnO_2	255	*Adv. Funct. Mater., 2025, e17063.*
H^+-LSE_xO	270	*J. Power Sources, 2025, 644, 237084.*
MoO_3@NF	288	*Int. J. Hydrogen Energy, 2025, 127, 137-146.*
Ni_5Fe-CNT	301	*Molecules, 2025, 30, 208.*
FeCoNiCuYP/C	259	*Adv. Mater., 2025, 37, 2410295.*
Co_2P/FeP	257	*J. Mater. Chem. A, 2024, 12, 31518-31525.*
$(Ni_{87}Fe_4Cr_9)_{78}Si_8B_{14}$	295	*Int. J. Hydrogen Energy, 2024, 92, 174-185.*
CCO5	337	*J. Electroanal. Chem., 2024, 973, 118677.*
NiBDC-A	293	*Small, 2024, 20, 2407328.*
P-$CoMoO_4$-Co_3O_4	279	*Nanoscale, 2024, 16, 18076-18085.*
NiCo-LDH/CN/AgPO	289	*J. Alloys Compd., 2024, 1004, 175860.*
Mo,Cl-Ni_3S_2	**254**	***This study***

Table S2 A summary of EGOR properties of Mo,Cl-Ni_3S_2 and state-of-the-art TM-based catalysts.

Catalyst	Current density (mA cm^{-2})	Potential (V vs. RHE)	Electrolyte	References
$Cu_{0.5}Co_{0.5}SnO_{3.17}$	10	1.46	1 M KOH + 0.3 M EG	*J. Colloid Interface Sci., 2025, 698, 138018.*
PdFe/N-CNTs	10	1.43	1 M KOH + 0.3 M EG	*J. Mater. Chem. A, 2024, 12, 15984.*
A-CoFeNi	10	1.36	1 M KOH + 0.3 M EG	*Chem. Eng. J., 2024, 498, 155472.*
Mo-Ni_2P/NF	50	1.37	1 M KOH + 0.3 M EG	*Appl. Catal. B: Environ., 2026, 386, 126372.*
$NiCu_{60s}$/NF	100	1.52	1 M KOH + 0.3 M EG	*ACS Catal., 2024, 14, 5314–5325.*
NiCu/NF	100	1.45	1 M KOH + 0.3 M EG	*ACS Catal., 2024, 14, 5314.*
Ni-Fe_3Se_4/NF	100	1.37	1 M KOH + 0.3 M EG	*J. Mater. Chem. A, 2026, 14, 1923.*
NiCe@NiTe	100	1.38	1 M KOH + 0.3 M EG	*J. Mater. Chem. A, 2026, 14, 3591–3604.*
MoS_2-(Ni,Fe)S_2@WC	100	1.41	1 M KOH + 0.3 M EG	*Chem. Eng. J., 534 (2026) 175122.*
Ni/Ni_3N_{1-x}	100	1.38	1 M KOH + 0.3 M EG	*J. Mater. Chem. A, 2024, 12, 15772–15780.*
2D-CoNi-PET	100	1.41	1 M KOH + 0.3 M EG	*Small, 2026, 22, e12758.*
Mo,Cl-Ni_3S_2	10 50 100	1.32 1.35 1.37	1 M KOH + 0.3 M EG	***This study***

Table S3 Calculated charge transfer resistance (R_{ct}) and solution resistance (R_s) of catalysts obtained from the Nyquist plot during the EIS experiments.

Catalyst	R_s (Ω)	R_{ct} (Ω)
Mo,Cl-Ni_3S_2	0.70	3.6
Mo-Ni_3S_2	0.76	6.2
Cl-Ni_3S_2	0.79	8.3
Ni_3S_2	0.82	29.4
NF	0.85	82.4

Table S4 The charge transfer resistance (R_{ct}) of Mo,Cl-Ni_2S_3 calculated from operando EIS data.

Potential (V vs. RHE)	EGOR (Ω)	OER (Ω)
1.10	1168.15	2243.74
1.15	717.82	1079.41
1.20	353.46	723.82
1.25	155.41	506.66
1.30	92.63	421.64
1.35	19.86	148.26
1.40	2.51	57.65
1.45	1.17	55.81
1.50	1.12	50.21
1.55	0.99	8.31

References

1 J. Sun, B. Shi, S. Dai, L. Chu, H. Wang and M. Huang, *ACS Catal.*, 2024, **15**, 529-542.
2 P. Chen, X. Zhang, C. Li, Y. Zhao, X. Chen, B. Wang and J. Wang, *Chem. Eng. J.*, 2026, **534**, 175166.
3 H. Zhou, Y. Ren, Z. Li, M. Xu, Y. Wang, R. Ge, X. Kong, L. Zheng and H. Duan, *Nat. Commun.*, 2021, **12**, 4679.
4 Y. Yang, M. Jiang, Y. Wang, Y. Zhang, Y. Wu and D. Wu, *Mater. Today Phys.*, 2025, **56**, 101775.
5 Z. Li, P. Wang, G. Han, S. Yang, S. Roy, S. Xiang, J. D. Jimenez, V. K. R. Kondapalli, X. Lyu, J. Li, A. Serov, R. Li, V. Shanov, S. D. Senanayake, A. I. Frenkel, P. M. Ajayan, Y. Sun, T. P. Senftle and J. Wu, *Nat. Commun.*, 2025, **16**, 4850.
6 M. Du, Y. Zhang, S. Kang, C. Xu, Y. Ma, L. Cai, Y. Zhu, Y. Chai and B. Qiu, *Small*, 2023, **19**, 2303693.
7 M. Du, Y. Zhang, S. Kang, C. Xu, Y. Ma, L. Cai, Y. Zhu, Y. Chai, B. Qiu, *Small*, 2023, **19**, 2303693.
8 M. Wang, B. Zhang, J. Ding, F. Zhang, R. Tu, M.T. Bernards, Y. He, P. Xie, Y. Shi, *Small*, 2022, **18**, 2105741.
9 F. Liu, X. Gao, R. Shi, E.C.M. Tse, Y. Chen, *Green Chem.*, 2022, **24**, 6571-6577.
10 M. Song, Y. Wu, Z. Zhao, M. Zheng, C. Wang, J. Lu, *Adv. Mater.*, 2024, **36**, 2403234.
11 J. Sun, B. Shi, S. Dai, L. Chu, H. Wang, M. Huang, *ACS Catal.*, 2024, **15**, 529-542.
12 J. Qi, J. Li, X. Meng, Z. Jiang, Z. Wang, Y. Ma, H. Zou, Y. Du, Z. Lin, J. Qiu, *Adv. Energy Mater.*, 2025, **15**, e04208.
13 W. Wang, X. He, Z. Tu, D. Xiong, S. Dong, T. Zhang, D. Wu, J. Wang, Z. Chen, *ACS Catal.*, 2025, **15**, 9574-9583.
14 W. He, H. Liu, J. Cheng, Y. Li, C. Liu, C. Chen, J. Zhao, H.L. Xin, *ACS Appl. Mater. Interfaces*, 2022, **14**, 6869-6875.
15 C. Yan, E. Han, X. Yang, K. Hu, H. Xu, Y. Li, Y. He, S. Lu, *Ceram. Int.*, 2023, **49**, 14155-14165.
16 Z. Chen, R. Zheng, T. Bao, T. Ma, W. Wei, Y. Shen, *Nano-Micro Lett.*, 2023, **15**, 210.